Available online at www.sciencedirect.com
SCIENCE DIRECT®
Journal of Nuclear Materials 325 (2004) 79–86
journal of nuclear materials
www.elsevier.com/locate/jnucmat

Hydrogen embrittlement of a V4Cr4Ti alloy evaluated by different test methods

Jiming Chen [a,b,*], Takeo Muroga [c], Shaoyu Qiu [b], Ying Xu [a], Ying Den [a], Zengyu Xu [a]

[a] Southwestern Institute of Physics, P.O. Box 432, Chengdu 610041, People's Republic of China
[b] National Key Laboratory of Nuclear Fuel and Materials, P.O. Box 436, Chengdu 610041, People's Republic of China
[c] National Institute for Fusion Science, Oroshi, Toki, Gifu 509-5292, Japan

Received 1 March 2002; accepted 31 October 2003

Abstract

The hydrogen embrittlement behavior of a V4Cr4Ti alloy (NIFS-Heat 2) has been studied using tensile tests, impact tests and J integral tests. Hydrogen in the alloy was high up to 310 wppm by exposures in a hydrogen atmosphere. The alloy showed different sensitivities to the hydrogen embrittlement in the tests. Hydrogen-induced solid solution hardening occured but caused slight loss in the ductility of the alloy before 215 wppm H in the tensile test. However, the impact toughness, J_{1c} and the tearing modulus (T_{mat}) decreased largely with increasing hydrogen concentration, indicated that the critical hydrogen concentration required to embrittle the alloy might be lower than 130 wppm. The fracture characteristics varied a lot for the different specimens. All these differences were thought being resulted from the stress concentration and the stress assisted hydrogen diffusion in the compact tension specimen and in the necking area of a tensile specimen.

PACS: 28.52.Fa; 61.82.Bg; 81.40.Np; 81.70.Bt; 46.30.Nz

1. Introduction

Hydrogen embrittlement is one of the key issues for vanadium alloys in their fusion applications. Many researches use tensile tests to study the embrittlement behaviors [1–4]. One reported that the US heat V4Cr4Ti alloy (#832665) could bear at least 400 wppm hydrogen without significant loss in the tensile elongation [5]. It seems that hydrogen embrittlement is not a serious concern for the alloy unless it has high oxygen concentration [4,5]. There are other ways to assess the brittleness or toughness of an alloy. In recent years, impact testing and fracture toughness testing have been more widely used to evaluate the mechanical properties of the large heat vanadium alloys, including those after neutron irradiations [6–8]. However, they were rarely found to be used for the assessment of the hydrogen embrittlement. Considering the engineering importance, the hydrogen-induced loss in fracture toughness and impact toughness should be more studied for the vanadium alloys. The effects of the pre-crack or notch in the specimen on the fracture behavior could be understood through the study.

There are more and more efforts from many countries on the development of vanadium alloys in large scale [9]. Following the production of a 500 kg scale V4Cr4Ti in US several years ago, National Institute for Fusion Science (NIFS) in Japan has recently developed a 166 kg heat V4Cr4Ti alloy (NIFS-heat 2) [10]. Property evaluation of the alloy has been carried out with international collaborations under the coordination of

* Corresponding author. Tel.: +86-28 8293 2225; fax: +86-28 8293 2202.
E-mail address: chenjm@swip.ac.cn (J. Chen).

0022-3115/$ - see front matter © 2003 Elsevier B.V. All rights reserved.
doi:10.1016/j.jnucmat.2003.10.014

IEA (International Energy Agency). Southwestern Institute of Physics (SWIP) in China has joined the program on the hydrogen embrittlement resistance evaluation of the alloy. Tensile tests, impact tests and J_{1c} tests have been performed and the results will be given in the present paper.

2. Experimental

2.1. Material and the test procedure

The test material was a V4Cr4Ti alloy produced in Japan (NIFS-Heat 2). Its chemical compositions were listed in Table 1. The alloy plates had ever taken a cold rolling with about 95.5% CW before the final annealing treatment that was conducted at 1000 °C for 2 h in vacuum. The plates were in two thicknesses of 1.9–6.6 mm. Fig. 1 showed the microstructure of the thick plate in a cross-section perpendicular to the rolling direction. There were two kinds of grains, the bigger one in size of ~13 μm and the much smaller one in size of ~2.5 μm on average. The thinner plate was used for fabrication of tensile specimens and the thick one for both the half-size charpy impact specimens and the compact tension (CT) specimens for J_{1c} testing in this experiment. Fig. 2 showed the configurations and the size of the specimens. All specimens have their longitude parallel to the rolling direction. V notch in 45° angle was placed on the thin plane of the impact specimen with a depth of 2 mm and a root radius of 0.25 mm.

Table 1
Chemical compositions of the NIFS heat V4Cr4Ti alloy (wt%)

Cr	Ti	C	N	O	H
4.03	3.73	0.0062	0.0084	0.022	0.0024

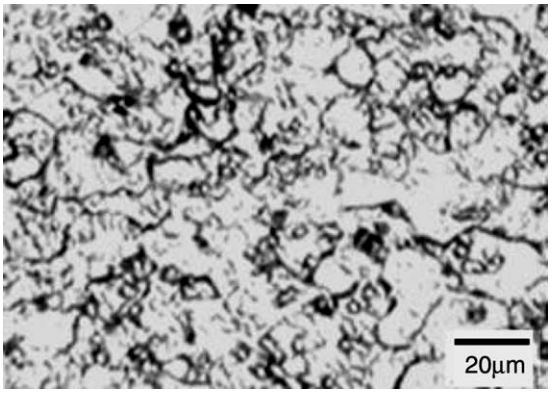

Fig. 1. An optical photo showing the microstructure of the alloy.

All specimens were placed in the vacuum chamber of a hydrogenating device to charge hydrogen before any test. At first, they were degassed at 420 °C for 10 min in a vacuum of $\sim 2\times10^{-3}$ Pa. Then the temperature was increased to 700 °C for hydrogen charging. High purity hydrogen gas (99.9999%) was admitted through a controllable leak valve while the vessel was being evacuated. Hydrogen concentration of the specimens was controlled by the flow rate of the hydrogen gas and the time of the admittance. Finally, an equilibrium heat treatment was conducted at the temperature for 2 h in the same vessel without the admittance of the hydrogen gas. Vacuum valve on the outlet duct was closed and the vacuum pump was powered off during the heat treatment to prevent the hydrogen in the specimens from desorption. As a result, the vacuum decreased and oxygen uptake became more obvious for all of the specimens. The measured results showed that the oxygen concentration of the specimens reached to 300–400 wppm after the treatment. Some specimens were treated in the same process but without the admittance of hydrogen to investigate its effects on the tensile properties of the alloy. Table 2 showed that the strength of the alloy was slightly increased but the total elongation did not change much.

Hydrogen concentration in the specimens was measured using a RH404 type hydrogen-measuring device that was made by the Leco Co. in United States. Placed in a graphite crucible in the device, the alloy sample was blown with argon gas to remove the other gases adhered to the sample surface. Then the sample was heated to ~1800 °C to release all of the hydrogen in the sample. The hydrogen was then brought out by a flowing argon gas to a thermal conductivity-detecting chamber where the hydrogen content was measured. The measured results showed that the maximum hydrogen concentration of the charged specimens was high up to 310 wppm.

Mechanical property tests were performed at room temperature. The charpy impact test had a velocity of 5 m/s. Both tensile test and J_{1c} test were performed on a MTS810 test machine with a strain rate of $\sim 4\times10^{-4}$ s^{-1} and a displacement rate of 0.1 mm/min, respectively. The CT specimens were pre-cracked on the same machine using a fatigue test method before the hydrogen charging. The pre-fatigue crack length (a_0) was from 9.44 to 10.08 mm, giving the ratio of a_0/W in the range of 0.59–0.63. A single-specimen method was used to measure the J integral. The specimen was unloaded after certain crack extension. Then it was placed in liquid nitrogen to get cooled to about −196 °C and forced to fracture thoroughly. The initial crack length and the crack propagation distance at the unload point were then measured under an optical microscope. After all of the tests, the fracture surface was observed under a scanning electron microscope (SEM).

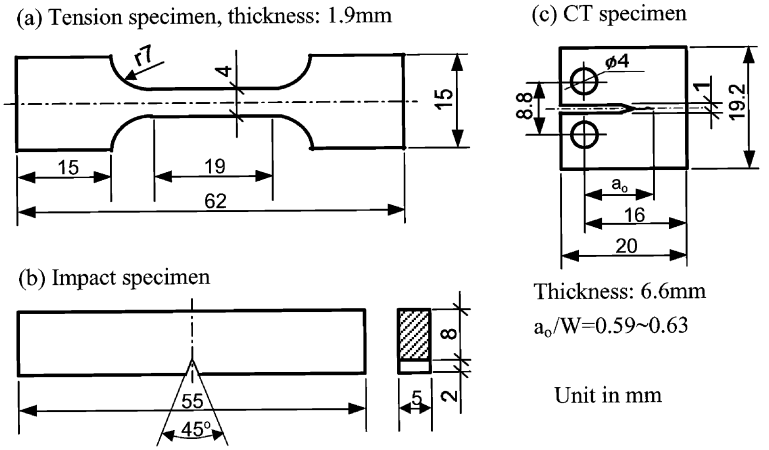

Fig. 2. The configuration and size of the test specimens.

Table 2
The tensile properties of the as-received alloy and the one with 700 °C heat treatment[a]

State	σ_y (MPa)	σ_{UT} (MPa)	δ (%)
As-received	306/308	390/394	30/34
700 °C pre-heated	305.8/313.5	399.3/400.6	31.2/32.3

[a] σ_y: yield strength, σ_{UT}: ultimate tensile strength, δ: total elongation.

2.2. Evaluation of the J_{Ic} and the T_{mat}

J was calculated according to Eq. (1)

$$J = \frac{A}{Bb} f(a/W), \tag{1}$$

where A is the area under the load–displacement curve; a is the crack length; b is the width of the uncracked ligament; B and W are the thickness and the width of the CT specimen, respectively;

$$f(a/W) = 2(1+\alpha)/(1+\alpha^2), \tag{2}$$

where

$$\alpha = [(2a/b)^2 + 2(2a/b) + 2]^{1/2} - [(2a/b) + 1]. \tag{3}$$

The tearing modulus of the alloy (T_{mat}) was defined as follows:

$$T_{mat} = \frac{E}{\sigma_0^2} \cdot \frac{dJ}{da}, \tag{4}$$

where E is Young's modulus of the alloy, σ_0 is flow stress (averaged by ultimate and yield strength); dJ/da is the slope of the J–Δa curve and Δa is the crack extension. Substituting a and b in Eq. (1) with a_0 and b_0 (the initial crack length and the initial ligament width), we got a J integral called J_Q. If it meets the following validity condition then it is the fracture toughness of the alloy (J_{Ic}).

$$a_0, b_0, B \geqslant 25 J_Q/\sigma_y, \tag{5}$$

where σ_y is the yield strength of the alloy.

In order to get T_{mat}, we must know the crack extension in the test to get the J–Δa curve. Here an assumption was made that the load (P) beyond the maximum load (P_{max}) point at the load–displacement curve is proportional to the flow stress of the alloy and has a functional relationship with b/w as Eq. (6).

$$P = g(b/W) \cdot \sigma_0. \tag{6}$$

A set of (P, b) data at the maximum load point and the unload point could be obtained from the test. The data was plotted in Fig. 3(a), which showed the relation between P/σ_0 and b/W. According to the data, the best-fitted curve is:

$$g(b/W) = 22.22(b/W)^{1.5244}. \tag{7}$$

Thus for a specimen

$$\frac{P}{P_{max}} = \left(\frac{b}{b_0}\right)^{1.5244}. \tag{8}$$

The uncracked ligament width at any point on the load–displacement curve could thus be generated and so did the crack extension since $\Delta a = b_0 - b$. This method is just like the conventional load-drop method [11] but corrected using the measured crack extension at the unload point. Fig. 3(b) showed one of the

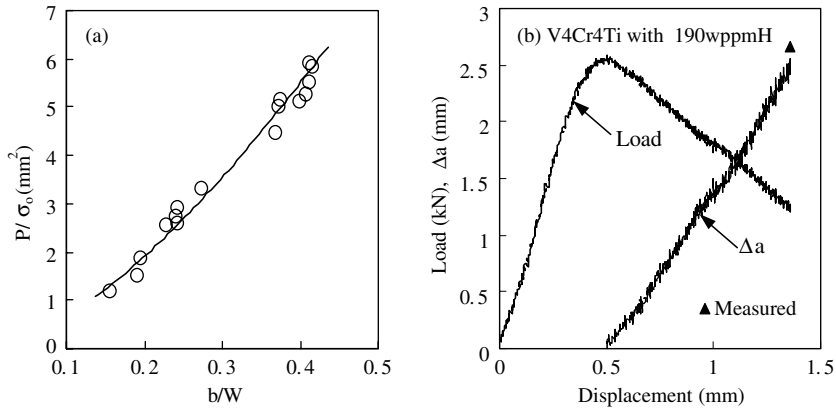

Fig. 3. The dependence of the P/σ_0 on b/W for all CT specimens (a) and the load–displacement curve along with the calculated crack extension for the CT specimen with 190 wppm hydrogen (b).

load–displacement curves and the calculated crack extension. It was a little lower than the actually measured one at the unload point.

3. Results and discussion

3.1. Tensile test

Fig. 4 showed the tensile properties of the alloy with the change of the hydrogen concentration. In the range from 24 (the original hydrogen concentration of the as-received alloy) to 215 wppm H, the hydrogen induced solid solution hardening, both the yield strength and the ultimate tensile strength increased in a similar rate. The total elongation exhibited a negative dependence on the hydrogen. It decreased with the hydrogen monotonically from ~31.7% to ~17% in the range. The ductility of the alloy was entirely lost at 310 wppm H, indicating a complete brittle fracture of the specimen. The critical hydrogen concentration required to embrittle the alloy in this static tension loading condition is thus between 215 and 310 wppm. On the other hand, the uniform elongation behaved differently. It had a value of ~15% and was nearly unchangeable with the change of the hydrogen before 215 wppm. It seemed that the hydrogen effect on the ductility was solely to reducing the non-uniform deformation in the necking area.

Natesan and Soppet [13] reported that the critical hydrogen concentration required to embrittle the US V4Cr4Ti alloy (heat #832665) is about 360 wppm based on their tensile test results. The alloy had an oxygen concentration of 310 wppm. Another report from DiStefano et al. [5] concluded that the concentration is more than 500 wppm according to their studies. Also found was the strong effect of the oxygen concentration on the behavior. With 850 wppm O the alloy would be embrittled by ~90 wppm H. In this experiment, the critical hydrogen concentration was a little lower than that for the US heat. The reason must be the relatively

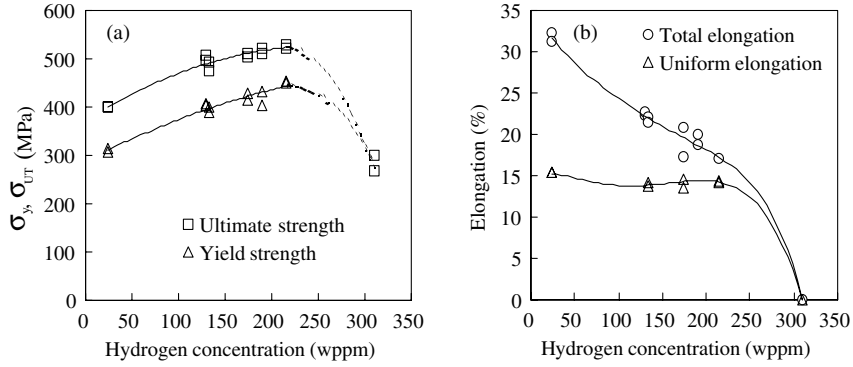

Fig. 4. The tensile test properties of the NIFS-V4Cr4Ti alloy with hydrogen at room temperature, (a) tensile strength and (b) elongation.

higher oxygen concentration in those hydrogen charged specimens. In a study reported by Rohrig et al. [2], just like what was found here, the uniform elongation of their studied V4Cr4Ti alloy was not affected by the hydrogen before ~450 wppm H while the total elongation decreased. But they have not given the reason. Here it was thought being caused by the stress assisted hydrogen diffusion around the necking area, which suppressed the necking and reduced the non-uniform deformation. This will be discussed in detail later in this paper in combination with the fracture mechanism analysis.

3.2. Impact test and J_{1c} test

Fig. 5(a) showed that the absorbed energy of the specimens decreased drastically with increasing hydrogen concentration in the impact process. At 130 wppm H the energy is less than half of that for the non-hydrogen charged specimens. It could be concluded from the figure that more than 190 wppm H is needed to bring about complete brittle fracture. The energy absorbed in the impact process should consist of two parts: one was the energy required to initiate a crack in the specimen, which showed the capability of the alloy against the crack initiation. Another was the energy needed to drive the crack to propagate successively. It must be large enough to overcome the crack extension resistance. So these two parts have different meaning for the alloy. Here the impact test results could not separate the two parts. It is necessary to evaluate the two parts separately by measuring the fracture toughness of the alloy and its crack propagation resistance indicated by the tearing modulus.

J_{1c} test result was shown in Fig. 5(b). A specimen compliance change rate method [12] was used to determine the crack initiation point and it was found that the point located at the maximum load point nearly for all of the specimens. The corresponding J integral was taken as J_{1c} when it meets the validity criterion of Eq. (5). All the data in the figure meets the criterion except that for the specimen without hydrogen charged, which, however, had much high J integral of 594.7 kJ/m^2, indicating that the as-received alloy was very tough. The figure showed that the alloy with more than 130 wppm hydrogen had much lower fracture toughness. J_{1c} was less than 50 kJ/m^2 and was little affected by the hydrogen concentration in the regime from 130 to 190 wppm. Accordingly, the critical hydrogen concentration to induce brittle crack propagation initially must be less than 130 wppm in the alloy with cracks. At 310 wppm H, complete brittle fracture happened with J_{1c} reaching to the lowest value of ~4 kJ/m^2.

Fig. 6 showed the hydrogen dependence of the tearing modulus. In opposite to the change of J_{1c}, T_{mat} almost decreased linearly with increasing hydrogen concentration and all in a low level less than 50. The tearing modulus is thus more sensitive to the hydrogen-induced embrittlement. It would drop to zero at 214 wppm H according to the line. Thoroughly brittle fracture will occur beyond this critical hydrogen concentration.

It is well known that hydrogen could decrease the binding force of the atoms in an alloy. Thus the crack could propagate more easily. So it seemed that the tearing modulus is directly related to the binding force and Fig. 6 indicated that the force decreased linearly with the hydrogen. Some researches showed that the ductility of another V4Cr4Ti alloy did not change much before a critical hydrogen concentration when the property was evaluated by tensile tests [1,2]. Obviously the tensile properties are less sensitive to hydrogen embrittlement than the tearing modulus. Therefore, J testing and the tearing modulus should preferentially

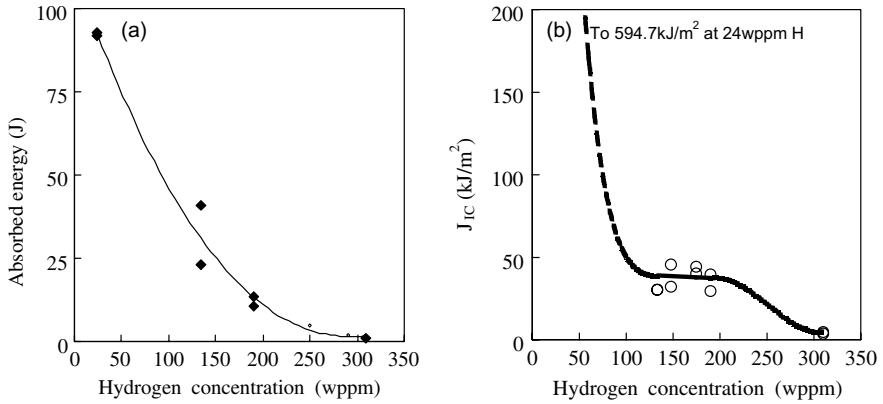

Fig. 5. The hydrogen concentration dependence of the (a) absorbed energy of the impact specimen and (b) J_{1c} for the V4Cr4Ti alloy. Test temperature: room temperature.

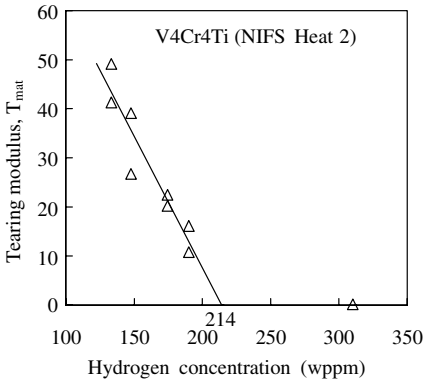

Fig. 6. Tearing modulus of the alloy at different hydrogen concentrations at room temperature.

be used to evaluate the hydrogen embrittlement of a material considering the possible crack in it.

3.3. SEM observation of the fracture surfaces

Fracture mechanism is analyzed to reveal the hydrogen embrittlement behavior of the alloy. SEM observation showed that ductile fracture with many dimples was the major feature for the non-hydrogen charged specimens, corresponding to the high ductility and toughness of the as-received alloy. However, with the hydrogen doped, the fracture changed much. Fig. 7 showed the fractographs of the specimens at a similar hydrogen level. It looks obviously different from each other in fracture mode. The tensile specimen had a quasi-cleavage fracture with many secondary cracks. CT specimen showed a typical cleavage fracture with a few tearing ridges in the initial cracked region, followed by the quasi-cleavage fracture with many secondary cracks as that appeared in the tensile specimen. Being quite different, ductile dimple fracture dominated the fracture surface of the impact specimen with a few cleavage fracture regions. Further observation revealed that both the amount of the secondary cracks in the tensile specimen and the dimples in the impact one decreased with the increase of the hydrogen concentration, but the fracture mode in the initial cracked region in the CT specimens was hardly affected by the hydrogen of less than 190 wppm in concentration. It may account for the non-affected J_{1c} in the hydrogen concentration range. At 310 wppm H, all fractured in transgranular cleavage but with an exception of the impact specimen in which there were still a few regions fractured in dimple characteristics (see Fig. 8).

3.4. The effects of stress concentration

Fracture mode may be affected by the strain constraint at the crack tip in the CT specimen due to the three-directional stresses. It greatly increased the yield strength of the matrix near the tip. As a result, it increased the plastic deformation resistance and the alloy became more sensitive to the hydrogen embrittlement.

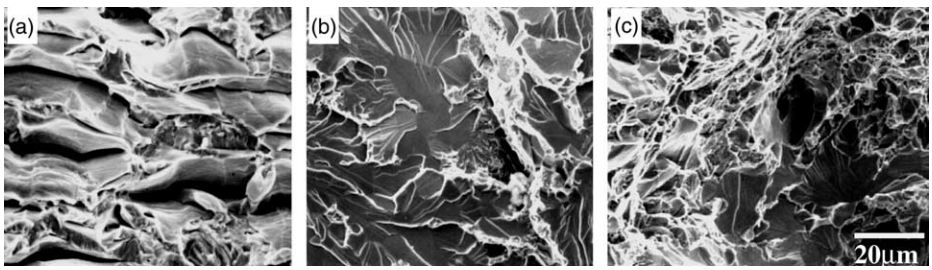

Fig. 7. SEM photos showing the fracture characteristics of the NIFS-V4Cr4Ti alloy with 174.5–190 wppm H for (a) tensile specimen, (b) CT specimen in the initial cracked region and (c) impact specimen.

Fig. 8. Fractographs of the fractured (a) CT specimen, (b) impact specimen and (c) tensile specimen at 310 wppm H.

As the crack propagated, the constraint became weaker due to the thinning of the uncracked ligament. Just as what was observed in SEM, followed by a cleavage fracture initially the fracture changed to the quasi-cleavage type due to the change of the constraint. For impact specimen, besides the similar but lower strain constraint near the notch, impact loading also has a tendency to embrittle the alloy. It was reasonable to think that the fracture of the impact specimen should be similar to that of the CT specimen. But the results showed that although the absorbed energy decreased drastically with the hydrogen concentration, the fracture surface contained a large portion of dimples even in the initial cracked region. So what made the different appearance of the fracture surface? And yet, it is still a question why the total elongation rather than the uniform elongation was reduced by the hydrogen. Stress concentration and the stress assisted hydrogen diffusion must be the main reason.

Hydrogen atom is very small and thus could have much high diffusion or migration rate in the alloy. If the stress in the specimen is not homogeneous, hydrogen will migrate to the high tension–stress region. In an early work reported by Yano et al. [14], it was found that the stress concentration at the Lüders band promoted the formation of hydride, which led to the loss of the capability of a V15Cr15Ti alloy against hydrogen embrittlement. Of course, the formation of the hydride is related to the hydrogen enrichment in the region. In the present tests, high stress concentration existed near the crack tip in the CT specimen. Calculated with the assumption of plane strain condition, the stress at the crack tip would reach to 700–800 MPa just before the initiation of the crack. The nearby hydrogen would diffuse into the region under the driving of the stress gradient. It is not known if there was hydride formed near the crack tip in the present test, but the hydrogen enrichment would certainly happen which increased the difficulty of the regional plastic deformation. Consequently, cleavage fracture became easier to take place. The fracture toughness was thus in much low value and was nearly unaffected by the hydrogen concentration from 130 to 190 wppm because of the hydrogen enrichment. The case in the necking area of a tensile specimen is just similar to this situation in the CT specimen but with weaker stress concentration. This should account for the strong effect of the hydrogen on the necking process rather than the uniform deformation. The stress assisted hydrogen diffusion would not occur in the impact specimen although there was also stress concentration ahead of the notch root, simply because of the fast loading process. The hydrogen in the specimen had scarcely time to diffuse into the high stress region when the fracture took place. It may be one of the main reasons for the large numbers of dimples on the fracture surface. The diffusion of the hydrogen was not measured in this study and may need further study of its effects on the hydrogen embrittlement behaviors considering the effects may be very strong.

4. Conclusions

NIFS-V4Cr4Ti alloy showed different properties against hydrogen embrittlement in different testing condition that could be concluded as follows:

(1) In the tensile test, the alloy could stands high level hydrogen concentration of more than 215 wppm without significant loss in the ductility. However, other test results showed that the fracture toughness J_{1c}, impact toughness and the tearing modulus of the alloy are strongly affected by the hydrogen and the critical hydrogen concentration required to embrittle the alloy may be less than 130 wppm.
(2) Hydrogen in the alloy caused solid solution hardening. Non-uniform plastic deformation rather than the uniform deformation was greatly suppressed by the hydrogen.
(3) Tearing modulus could reflect the effects of the hydrogen on the mechanical performance of the alloy more realistically. It decreased nearly linearly with increasing hydrogen concentration.
(4) Stress concentration and the stress assisted hydrogen diffusion near a crack tip or a notch root will enhance the hydrogen embrittlement of the alloy under static loading, leading to a much low fracture toughness at relatively lower hydrogen concentrations. The diffusion and its dependence on the stress gradient should be further studied.
(5) The fracture toughness of the alloy is less than 50 kJ/m^2, unaffected by the hydrogen concentration in the range from 130 to 190 wppm.

Acknowledgements

This work is conducted under the support of the Nature Science Foundation of China (project #50271025). The author would like to thank Dr Chen Yong and Mr Liang Bo in NPIC for their help in the tests.

References

[1] K. Aoyagi, E.P. Torres, T. Suda, S. Ohnuki, J. Nucl. Mater. 283–287 (2000) 876.
[2] H.D. Rohrig, J.R. DiStefano, L.D. Chitwood, J. Nucl. Mater. 258–263 (1998) 1356.
[3] J. Chen, S. Qiu, L. Yang, et al., J. Nucl. Mater. 302 (2002) 135.

[4] J.R. DiStefano, J.H. DeVan, D.H. Rohrig, L.D. Chitwood, J. Nucl. Mater. 273 (1999) 102.
[5] J.R. DiStefano, B.A. Pint, J.H. DeVan, et al., J. Nucl. Mater. 283–287 (2000) 841.
[6] H.D. Rohrig, M. Rieth, et al., J. Nucl. Mater. 283–287 (2000) 498.
[7] H. Tsai, T.S. Bray, H. Matsui, M.L. Grossbeck, et al., J. Nucl. Mater. 283–287 (2000) 362.
[8] H. Li, R.J. Kurtz, R.H. Jones, J. Nucl. Mater. 258–263 (1998) 1386.
[9] R.J. Kurtz, K. Abe, V.M. Chernov, et al., J. Nucl. Mater. 283–287 (2000) 70.
[10] T. Muroga, T. Nagasaka, K. Abe, V.M. Chernov, H. Matsui, D.L. Smith, Z.-Y. Xu, S.J. Zinkle, J. Nucl. Mater. 307–311P1 (2002) 547.
[11] J.A. Kapp, in: Fracture Mechanics: Sixteenth Symposium, ASTM STP 868, 1985, p. 281.
[12] T. Kobayashi, I. Yamamoto, M. Niinomi, Eng. Fract. Mech. 24 (1986) 773.
[13] K. Natesan, W.K. Soppet, J. Nucl. Mater. 283–287 (2000) 1316.
[14] S. Yano, M. Tada, H. Matsui, J. Nucl. Mater. 179–181 (1991) 779.